Title

Stabilization of Cyclin-Dependent Kinase 4 by Methionyl-tRNA Synthetase in p16INK4a-Negative Cancer

Journal

ACS Pharmacology & Translational Science, 1(1)

ISSN

2575-9108

Authors

Kwon, Nam Hoon
Lee, Jin Young
Ryu, Ye-lim
et al.

Publication Date

2018-09-14

DOI

10.1021/acsptsci.8b00001

Peer reviewed

ACS Pharmacology & Translational Science

Article

Cite This: ACS Pharmacol. Transl. Sci. 2018, 1, 21−31

Stabilization of Cyclin-Dependent Kinase 4 by Methionyl-tRNA Synthetase in p16^{INK4a}-Negative Cancer

Nam Hoon Kwon,[†,‡,○] Jin Young Lee,[†,○] Ye-lim Ryu,[†] Chanhee Kim,[†] Jiwon Kong,[†] Seongeun Oh,[†] Beom Sik Kang,[§] Hye Won Ahn,[†] Sung Gwe Ahn,[∥] Joon Jeong,[∥] Hoi Kyoung Kim,[†] Jong Hyun Kim,[†] Dae Young Han,[†] Min Chul Park,[†] Doyeun Kim,[†] Ryuichi Takase,[⊥] Isao Masuda,[⊥] Ya-Ming Hou,[⊥] Sung Ill Jang,[#] Yoon Soo Chang,[#] Dong Ki Lee,[#] Youngeun Kim,[†] Ming-Wei Wang,[▽] Basappa,[¶] and Sunghoon Kim*[,†,‡]

[†]Medicinal Bioconvergence Research Center, Seoul National University, Suwon, 16229, Korea

[‡]Department of Molecular Medicine and Biopharmaceutical Sciences, Graduate School of Convergence Science and Technology, Seoul National University, Seoul, 08826, Korea

[§]School of Life Science and Biotechnology, Kyungpook National University, Daegu, 41566, Korea

[∥]Breast Cancer Center, Department of Surgery, Gangnam Severance Hospital, Yonsei University College of Medicine, Seoul, 03722, Korea

[⊥]Department of Biochemistry and Molecular Biology, Thomas Jefferson University, Philadelphia, Pennsylvania 19107, United States;

[#]Department of Internal Medicine, Gangnam Severance Hospital, Yonsei University College of Medicine, Seoul, 03722, Korea

[▽]The National Center for Drug Screening, Shanghai Institute of Materia Medica, Chinese Academy of Sciences, Shanghai, 201203, China

[¶]Laboratory of Chemical Biology, Department of Chemistry, Bangalore University, Palace Road, Bangalore, 560 001, India

Supporting Information

ABSTRACT: Although abnormal increases in the level or activity of cyclin-dependent kinase 4 (CDK4) occur frequently in cancer, the underlying mechanism is not fully understood. Here, we show that methionyl-tRNA synthetase (MRS) specifically stabilizes CDK4 by enhancing the formation of the complex between CDK4 and a chaperone protein. Knockdown of MRS reduced the CDK4 level, resulting in G0/G1 cell cycle arrest. The effects of MRS on CDK4 stability were more prominent in the tumor suppressor p16^{INK4a}-negative cancer cells because of the competitive relationship of the two proteins for binding to CDK4. Suppression of MRS reduced cell transformation and the tumorigenic ability of a p16^{INK4a}-negative breast cancer cell line *in vivo*. Further, the MRS levels showed a positive correlation with those of CDK4 and the downstream signals at high frequency in p16^{INK4a}-negative human breast cancer tissues. This work revealed an unexpected functional connection between the two enzymes involving protein synthesis and the cell cycle.

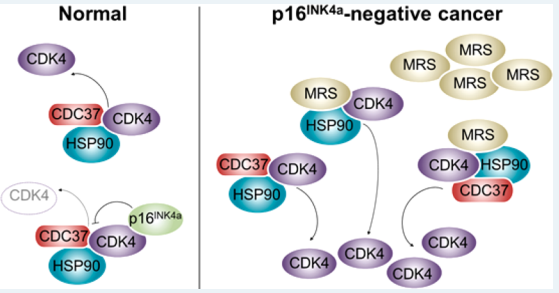

KEYWORDS: *cell cycle, methionyl-tRNA synthetase, CDK4, HSP90, p16^{INK4a}*

Cell cycle regulation requires the timely and successive activation and inactivation of different complexes between cyclins and cyclin-dependent kinases (CDKs). Among them, CDK4 in the form of a complex with cyclin D1, regulates the G1 to S transition and is critically involved in the decisions concerning growth and quiescence.[1] Active CDK4-cyclin D1 complexes phosphorylate Rb (Retinoblastoma) resulting in the dissociation of Rb from E2F.[2] Then, free E2F transcribes S phase-promoting genes, including cyclin E and cyclin A, and contributes the activation of cyclin E- and A-dependent CDKs. The single deletion of CDK4 resulted in little effect on the development of embryos and mammary glands, suggesting that it is not essential and replaceable in normal development and viability.[3,4] CDK4, however, is critical for the Ras-activated oncogenic transformation of MEFs (mouse embryonic fibroblasts), mammary tumorigenesis driven by Erbb2 or H-Ras, and the development of carcinogen- and Myc-induced skin cancers.[5−8] All these results suggest that CDK4 is a target for anticancer therapies, as indicated by the accelerated approval of the CDK4/6 inhibitor palbociclib for the treatment of advanced breast cancer.[9]

To ensure timely entry into the cell cycle and arrest in response to signal pathways, several factors are involved in

Received: February 15, 2018
Published: April 24, 2018

DOI: 10.1021/acsptsci.8b00001
ACS Pharmacol. Transl. Sci. 2018, 1, 21−31

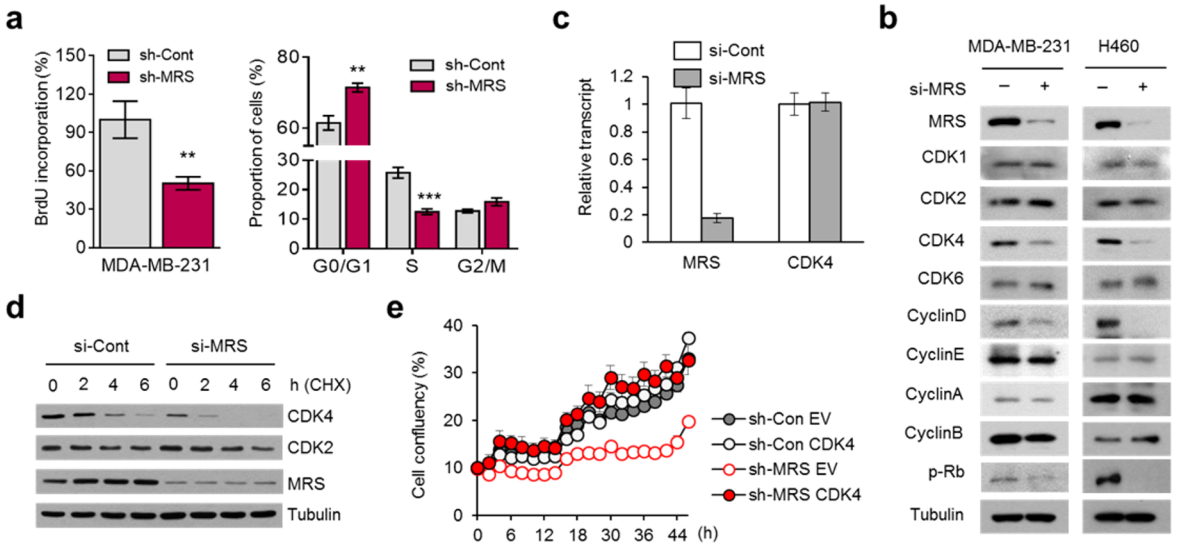

Figure 1. MRS suppression induces G1 cell cycle arrest via specifically reducing the CDK4 level and its downstream signaling. (a) BrdU levels (left) and cell cycle arrest (right) of MDA-MB-231 cells stably expressing sh-Control (sh-Cont) and sh-MRS (mean ± SEM, $n = 3$). (**) $P < 0.01$, (***) $P < 0.001$. (b) Levels of cell cycle-regulating proteins in cells transfected with si-MRS. (c) CDK4 transcript levels following treatment with si-MRS (mean ± SD, $n = 3$). (d) Specific reduction of CDK4 levels by si-MRS in A549 cells treated with cycloheximide (CHX, 20 μg/mL). (e) Growth of MDA-MB-231 cells stably expressing sh-MRS following CDK4 supplementation or EV (empty vector) transfection (mean ± SD, $n = 3$).

CDK4 regulation.[6,10] Tumor suppressor $p16^{INK4a}$, for example, interferes in the direct interaction between CDK4 and cyclin D1. Genetic deletions and hypermethylation in the promoter region of *CDKN2A*, which encodes $p16^{INK4a}$, have been observed in a large number of human cancers, including pancreatic, lung, and breast cancers.[1,5,10−12] The inactivation of $p16^{INK4a}$ in cancers leaves CDK4 uncontrolled, resulting in tumor progression. Therefore, finding a way to control CDK4 in $p16^{INK4a}$-negative cancers would be therapeutically meaningful. CDC37 (cell division cycle protein 37) and HSP90 (heat shock protein 90) enhance the proper folding and stabilization of CDK4 for the interaction with cyclin D1.[13,14] CDK4, when not bound by CDC37 and HSP90, is subjected to proteasome-dependent degradation.[13−16] However, it remains unclear how CDK4 is maintained at a high level in cancer cells and how the CDC37/HSP90 complex specifically recognizes CDK4 among more than 100 kinase clients.[13−16] Recent studies have shown that CDK4 stability can be maintained even under conditions that cause substantial dissociation of the CDC37/HSP90 complex,[15] suggesting that additional factor(s) may be involved in the control of CDK4.

Methionyl-tRNA synthetase (MRS) is an essential enzyme for translation. Human MRS forms a multi-tRNA synthetase complex (MSC) with other ARSs (aminoacyl-tRNA synthetases) and AIMPs (ARS-interacting multifunctional proteins) in the cytosol and charges methionyl-tRNA with methionine (Met).[17] Under oxidative stress, MRS incorporates more Mets in the growing polypeptide chains, which can serve as a scavenger of reactive oxygen species.[18,19] Upon UV irradiation, MRS is phosphorylated, resulting in the shutdown of tRNA charging and protein synthesis.[20] In addition to its important role in translation, MRS has also been shown to play a critical role in DNA repair, transcription, and rRNA synthesis in response to various cellular stimuli.[20−22] These reports suggest the functional flexibility of MRS in response to environmental stimuli and stresses.

Recently, several studies have reported *MARS* (gene encoding MRS) mutations as the novel cause of diseases.[23−25] According to van Meel et al., the compound heterozygous *MARS* mutations F370L and I523T caused a multiorgan phenotype in an infant. The significantly impaired MRS catalytic activity was identified as the cause of the illness, while the parents who were heterozygous for one of the mutations were healthy.[25] It also implies that hypomorphic MRS would not significantly affect the translational need required for normal life maintenance, provoking questions regarding how knockdown of MRS would affect global translation or cell phenotypes. To our surprise, the suppression of MRS had little effect on global translation but had a specific effect on the cell cycle, particularly on the transition from the G1 to S phase. This work thus investigated the working mechanism of MRS responsible for this unexpected cellular outcome.

RESULTS AND DISCUSSION

Effect of MRS Suppression on the CDK4 Level and Cell Cycle. To investigate the effect of MRS knockdown on cell proliferation, we prepared human breast MDA-MB-231 cancer cells stably expressing inducible short hairpin RNA (sh-RNA) and nonsmall cell lung carcinoma H460 cells transfected with small interfering RNA (si-RNA) specific to MRS and analyzed how MRS suppression affected cell proliferation and the cell cycle using BrdU (bromodeoxyuridine) incorporation and FACS (fluorescence-activated cell sorting) analyses. The MRS suppression significantly reduced the BrdU incorporation up to 50% (Figure 1a, left, and Supporting Information, Figure S1a) and induced G0/G1 cell cycle arrest (Figure 1a, right). Since MRS is an essential enzyme for protein synthesis, we expected that the reduction of cell growth would be attributed to decreased global translation. However, when we monitored global translation by Met incorporation assay, it was changed little by MRS knockdown, at least in the two tested cell lines (Figure S1b). It seems that the remaining MRS could still supply the Met-charged tRNA needed for translation under normal culture conditions. We further investigated whether a reduced MRS level would be sufficient to meet the translational

DOI: 10.1021/acsptsci.8b00001
ACS Pharmacol. Transl. Sci. 2018, 1, 21−31

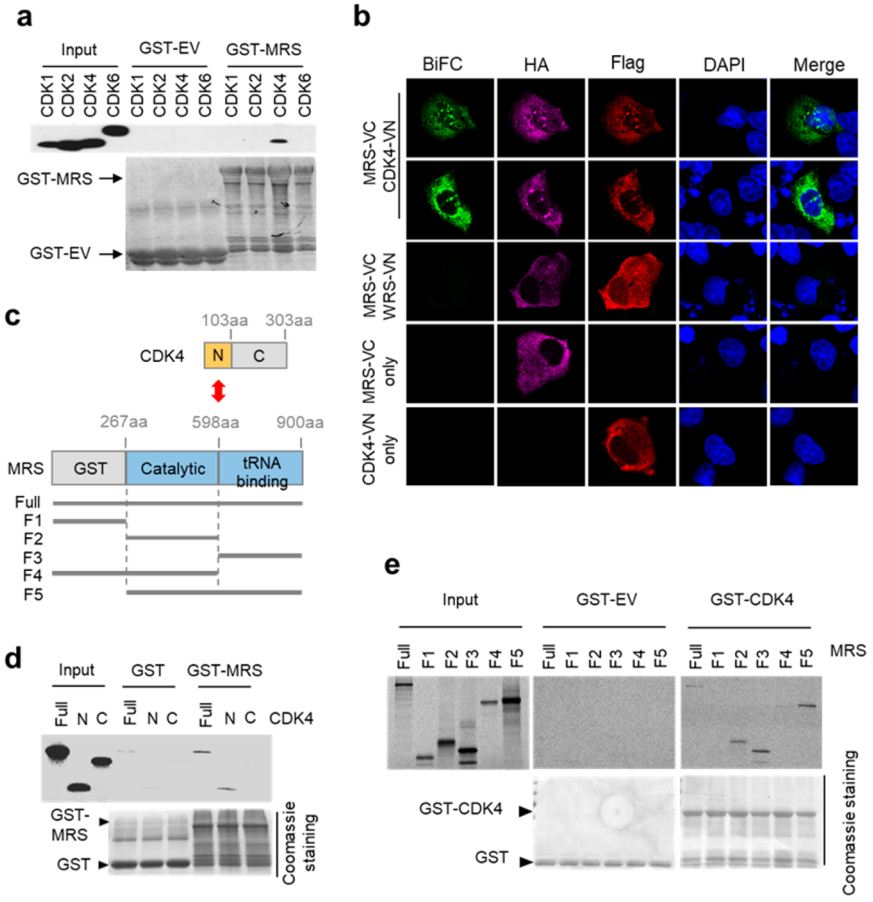

Figure 2. Catalytic and tRNA binding domains of MRS interact with the N-terminus of CDK4. (a) Coprecipitation of CDK4 with GST-MRS. (b) BiFC of green Venus fluorescence represents the interaction between MRS and CDK4 or between MRS and WRS (tryptophanyl-tRNA synthetase). H460 cells cotransfected with Flag-CDK4-VN and HA-MRS-VC were treated with MG132 (50 μM). Violet (Alexa Fluor 647) and red (Alexa Fluor 594) colors indicate the level of HA-MRS and Flag-CDK4 or WRS, respectively. Nuclei were stained with DAPI in blue. (c) Schematic depicting the domains involved in the MRS-CDK4 interaction. (d,e) *In vitro* pull-down assays revealing the CDK4 domains associating with GST-MRS (d) and MRS fragments associating with GST-CDK4 (e).

need even under starvation conditions. When we starved H460 cells for Met in serum-free media and performed the radioactive Met and Leu incorporation assays, global translation was reduced by MRS knockdown (Figure S1c). These results suggest that global translation is affected little by a shortage of MRS for a certain period under normal culture conditions. To verify the minor effect of MRS knockdown on global translation *in vivo*, we investigated the MRS level and global translation in various organs from *MARS* knockout mice, in which the transcription of the *MARS* gene is terminated prematurely due to the insertion of a gene trap cassette.[26] Actually, the MRS level in the homozygous mice did not completely disappear, but the level was reduced enough to represent the effect of MRS knockdown in almost all organs tested (Figure S2a). The reduced MRS level did not affect global translation *in vivo* (Figure S2b) as observed in the cell lines. In addition, the change in protein synthesis was negligible in the heterozygous and homozygous primary MEF cells, despite the decreased level of MRS (Figure S2c). There was also no significant difference in the body weights of mice regardless of MRS expression level (Figure S2d). These data strongly suggest that MRS knockdown did not affect translation under normal conditions even *in vivo*; therefore, we continued to monitor the effect of MRS on the cell cycle in the cancer cell lines.

To identify the link between MRS and the cell cycle in the cancer cell lines, we measured the change in the levels of representative CDKs and cyclins, which are directly involved in cell cycle control.[8] Under MRS suppression conditions, the levels of CDK4, cyclin D1, and the phosphorylation of their downstream effector retinoblastoma (pRb) at S780 were considerably reduced, with little change in the other protein levels (Figure 1b). Since cyclin D1 alone is prone to degradation because of its intrinsic instability,[27] we focused on the relationship between MRS and CDK4. Quantitative RT-PCR results showed that the mRNA level of CDK4 was not affected by si-MRS transfection (Figure 1c), suggesting that MRS regulates CDK4 at the protein level. When we monitored the effect of MRS on CDK4 half-life, the CDK4 level was proportionately changed by MRS knockdown or overexpression under cycloheximide (CHX) treatment (Figure 1d and Figure S3a).

The relationship between MRS and CDK4 for the control of cell proliferation was investigated via real-time monitoring of cell growth. MDA-MB-231 cells expressing sh-MRS showed reduced growth due to the reduction of MRS and CDK4 (Figure 1e and Figure S3b). Interestingly, the cell growth was restored to normal levels by the overexpression of CDK4 (Figure 1e), suggesting that these two proteins are functionally related in cell proliferation.

DOI: 10.1021/acsptsci.8b00001
ACS Pharmacol. Transl. Sci. 2018, 1, 21−31

Determination of Interacting Domains in MRS and CDK4. To understand how MRS stabilizes CDK4 levels, we investigated potential interactions between MRS and different CDKs using glutathione-S transferase (GST) pull-down assays. We found that among the tested CDKs, only CDK4 was specifically pulled down with GST-MRS (Figure 2a). To further confirm the cellular interaction between MRS and CDK4, we used the Venus bimolecular fluorescence complementation (BiFC) method,[20] in which H460 cells were cotransfected with the Venus C-terminal domain (VC) fused to MRS and the Venus N-terminal domain (VN) fused to CDK4, and found that the coexpression of the two constructs reconstituted Venus green fluorescence (Figure 2b). The concomitant green fluorescence was not produced by the coexpression of MRS and tryptophanyl-tRNA synthetase, proving that the green fluorescence resulted from the specific interaction between MRS and CDK4. The interaction between endogenous MRS and CDK4 was also confirmed via coimmunoprecipitation (Figure S3c).

Next, we performed GST pull-down and immunoprecipitation assays using various deletion fragments of MRS and CDK4 (Figure 2c). These results revealed that the catalytic and tRNA-binding domains of MRS interacted with the N-terminus of CDK4 (Figure 2c–e and Figure S3d). The F1 fragment, the GST-like domain of MRS, seemed to hinder the interaction between MRS and CDK4 because the F4 MRS fragment did not show an interaction even though it contains the catalytic domain (Figure 2c–e).

Effect of a Met Analogue (MA) on CDK4 Stability and the Cell Cycle. Since the MRS catalytic domain is involved in the interaction with CDK4 (Figure 2c–e), we tested whether an MA would work as an interaction inhibitor between MRS and CDK4. For this, we selected commercially available 13 MAs (Table S1) and tested their effects on the levels of CDK4 pathway molecules and MRS. Three compounds (MAs 6, 7, and 13) out of the 13 MAs significantly decreased the levels of CDK4, cyclin D1, and pRb, but not MRS (Figure S4a). Among them, MA6, Fmoc-Sec(Mob)–OH (FSMO) (Figure 3a), showed the best destabilization effect on the CDK4 pathway and was selected for further investigation. While FSMO at 25 μM significantly reduced CDK4, cyclin D1, and pRb levels (Figure 3b), it had little effect on global translation at this concentration (Figure 3c). FSMO inhibited the Met activation step and global translation at high concentrations over 100 μM (Figure 3c and S4b), and it showed specificity to MRS even at the 1 mM concentration (Figure S4c). The difference in the effective concentrations of FSMO on the reduction of CDK4 levels and on translation inhibition suggests that the effect of FSMO on the level of CDK4 does not result from the inhibition of translation. In the same context, the effect of FSMO on CDK4 levels could be considered as a chemical phenocopy of the effects of MRS knockdown (Figure 3d–f). The growth suppression caused by FSMO was restored by adding either MRS or CDK4, but not leucyl-tRNA synthetase (Figure 3g,h). These results suggest that MRS is specifically required for the stability of CDK4, and the catalytic domain of MRS is important for the interaction between the two, showing that an MA can regulate the MRS-mediated stability of CDK4 independent of MRS activity.

Binding of an MA to MRS and Its Effect on the Interaction between MRS and CDK4. We then determined whether FSMO affected the direct interaction between MRS and CDK4 by *in vitro* pull-down assay. The amount of CDK4

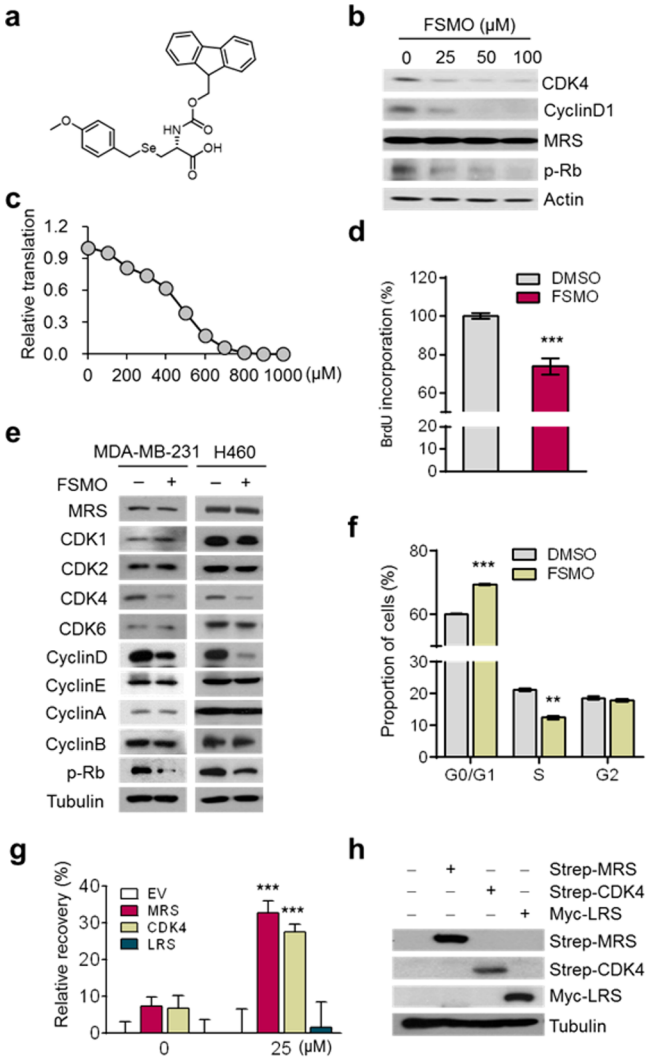

Figure 3. MRS inhibition induces G1 cell cycle arrest by specifically reducing the CDK4 level and its downstream signaling. (a) Structure of FSMO. (b,c) Dose-dependent effects of FSMO on the protein levels (b) and luciferase-based *in vitro* translation (c). (d) The effects of FSMO on cell proliferation measured by BrdU incorporation assay using 50 μM FSMO-treated H460 cells. (***) $P < 0.001$ (mean ± SD, $n = 3$). (e) Levels of proteins involved in the cell cycle were investigated in cells treated with 50 μM FSMO for 8 h. (f) The effects of FSMO on cell cycle progression were investigated by FACS analysis using 50 μM FSMO-treated H460 cells. (**) $P < 0.01$; (***) $P < 0.001$ (mean ± SD, $n = 3$). (g,h) Recovery effect of MRS, CDK4, and LRS on cell proliferation was analyzed by real-time monitoring in 25 μM FSMO-treated H460 cells using IncuCyte (g). The overexpression levels of MRS, CDK4, and LRS, which were transfected into H460 cells for the proliferation recovery test (g), were investigated via immunoblotting (h). (***) $P < 0.001$ (mean ± SEM, $n = 9$).

bound to MRS was decreased by the addition of FSMO in a dose-dependent manner (Figure 4a). FSMO also reduced the association between MRS and CDK4 in a coimmunoprecipitation experiment (Figure 4b). Considering that FSMO disturbed the Met activation step (Figure S4b), FSMO was expected to bind to the site of MRS, which is critical for the Met activation step. We thus introduced mutations at the H560 and K596 sites on MRS, which are crucial for Met binding and activation, respectively,[28,29] and determined how these mutations affected the interaction of MRS with CDK4.

DOI: 10.1021/acsptsci.8b00001
ACS Pharmacol. Transl. Sci. 2018, 1, 21–31

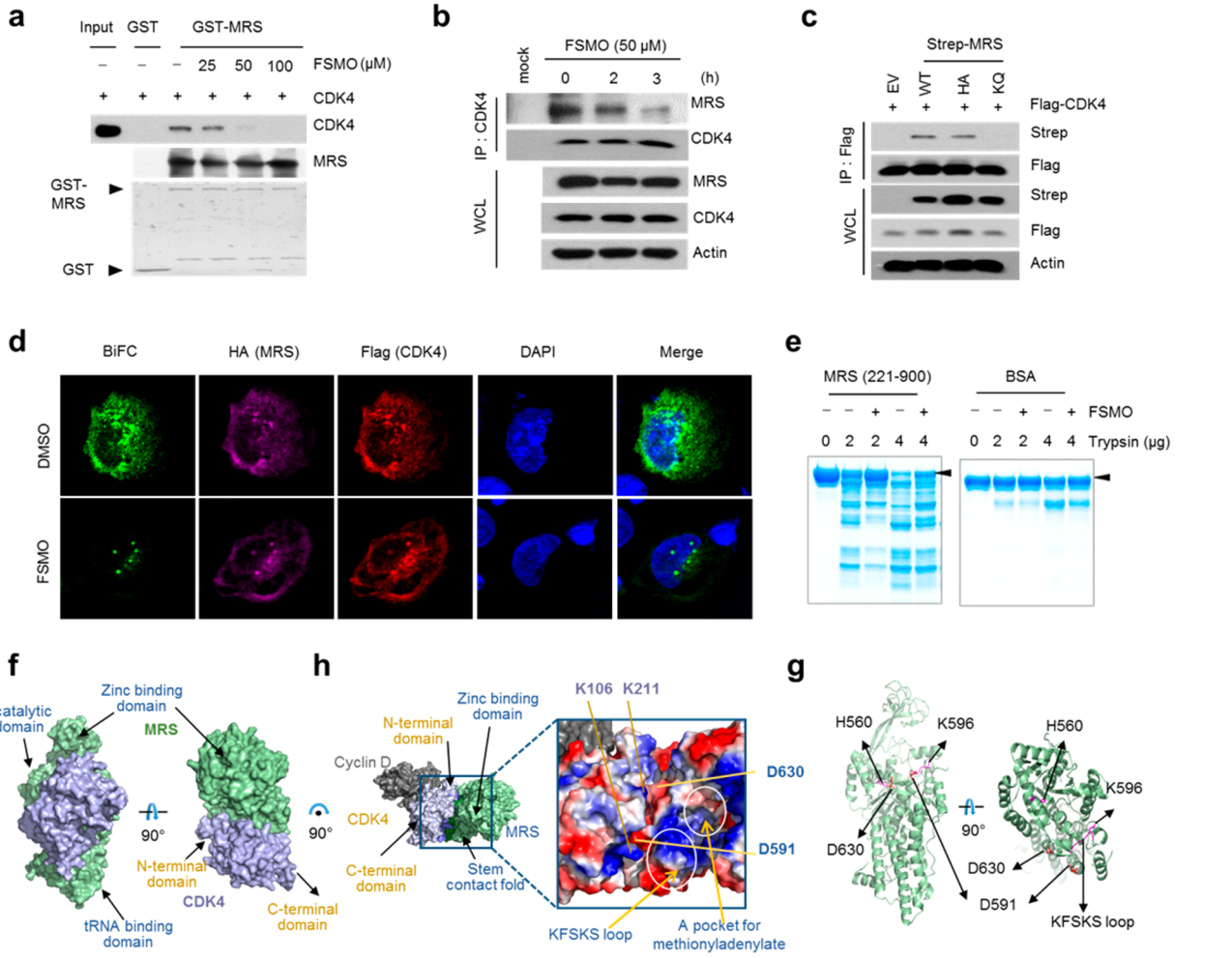

Figure 4. FSMO shares the binding site of MRS with CDK4. (a) Dose-dependent effect of FSMO on the MRS and CDK4 interaction. (b) Time-dependent effect of FSMO on the MRS and CDK4 interaction under MG132-treated conditions. (c) Co-immunoprecipitation assay to determine the interaction of Flag-CDK4 with Strep-MRS WT, H560A (HA) mutant, and K596Q (KQ) mutant. (d) Effect of FSMO (50 μM) on the reconstitution of Venus BiFC between Flag-CDK4-VN and HA-MRS-VC. MG132 (50 μM) was used to block CDK4 degradation. (e) Protective effect of FSMO against the trypsin digestion of MRS and BSA (bovine serum albumin). Arrows indicate the intact MRS and BSA proteins. (f) Model of the complex of MRS and CDK4. CDK4 (light blue) interacts with the tRNA binding side of MRS (pale green). (g) Position of the residues used for the mutation studies in Figure S5c. The residues are presented as sticks, and MRS is shown as a ribbon in the same orientation in panel f. D591 and D630 are near the KFSKS loop (magenta) including K596, and H560 is far from the binding site for CDK4. (h) Binding interface for CDK4 in MRS includes motifs for its catalytic reaction. MRS binds to CDK4 at the side opposite to cyclin D1 (gray). The positively charged region (K106 and K211) in CDK4 interacts with the negatively charged region (D591 and D630) in MRS. The zinc binding domain was removed to show the catalytic side including the KFSKS loop in the boxed figure.

Although the H560A mutant MRS associated with CDK4 similar to the wild type (WT), the K596Q mutant, which has the mutation on the second K in the KMSKS conserved motif (KFSKS in MRS), lost the CDK4 binding ability (Figure 4c). In addition, the CDK4 level was stabilized by the over-expression of the WT and H560A mutant, but not of the K596Q mutant, under CHX treatment (Figure S5a). We confirmed the effect of FSMO on the interaction between MRS and CDK4 by BiFC assay. FSMO reduced the green fluorescence signals (Figure 4d), further supporting its inhibitory effect on the cellular interaction between MRS and CDK4. We also performed a DARTS (drug affinity responsive target stability) assay to determine the masking effect of FSMO on the trypsinization of MRS and observed that the proteolytic cleavage of MRS was protected by FSMO based on the amount of intact MRS protein (Figure 4e). We performed a docking study with the crystal structures of MRS (PDB ID 5GL7) and CDK4 complexed with cyclin D1 (PDB ID 2W96) based on the results of *in vitro* pull-down assays (Figure 4f,g). In the docking model, the prominence and depression pattern on the tRNA binding domain of MRS matched that on CDK4. In the prominence area, the negatively charged residues D591 and D630 from MRS and E7 and E11 from CDK4 seemed to be critical for the interaction with the positively charged residues on the depressed area in the proteins (Figure 4h and Figure S5b). We mutated these residues on MRS and CDK4 and investigated the interaction between the two. As expected, the dual mutant (MT), in which D591 and D630 on MRS were substituted with Arg, reduced its association with CDK4 as did the E7R and E11R CDK4 mutant (Figure S5c), supporting the docking model. The MRS D591 and D630 residues are expected to respectively interact reciprocally with the K106 and K211 residues on CDK4 (Figure 4h), implying that some parts of the C-terminal domain of CDK4 may also be involved in the

DOI: 10.1021/acsptsci.8b00001
ACS Pharmacol. Transl. Sci. 2018, 1, 21−31

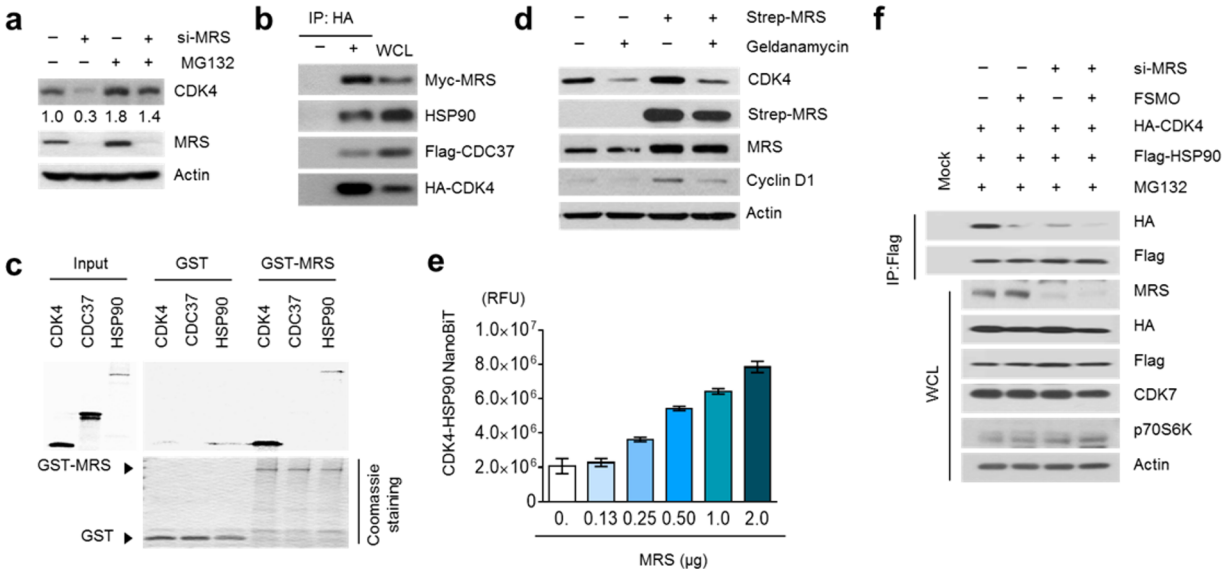

Figure 5. MRS facilitates CDK4−HSP90 complex formation and stabilizes CDK4. (a) H460 cells transfected with either si-Control or si-MRS were treated with a proteasome inhibitor (MG132). Relative levels of CDK4 were quantified using ImageJ. (b) MRS, CDC37, HSP90, and CDK4 were transfected into H460 cells, and their interaction was investigated. (c) Association of MRS with CDK4, HSP90, or CDC37 was investigated via *in vitro* pull-down assay. (d) Effect of geldanamycin (1 μM) on CDK4 in MRS-overexpressing H460 cells. (e) Effect of MRS on the interaction between CDK4 and HSP90 measured by reconstitution of nanoluciferase luminescence. (f) H460 cells were treated with FSMO and si-MRS in combination, and their effect on the interaction between overexpressed HSP90 and CDK4 was investigated.

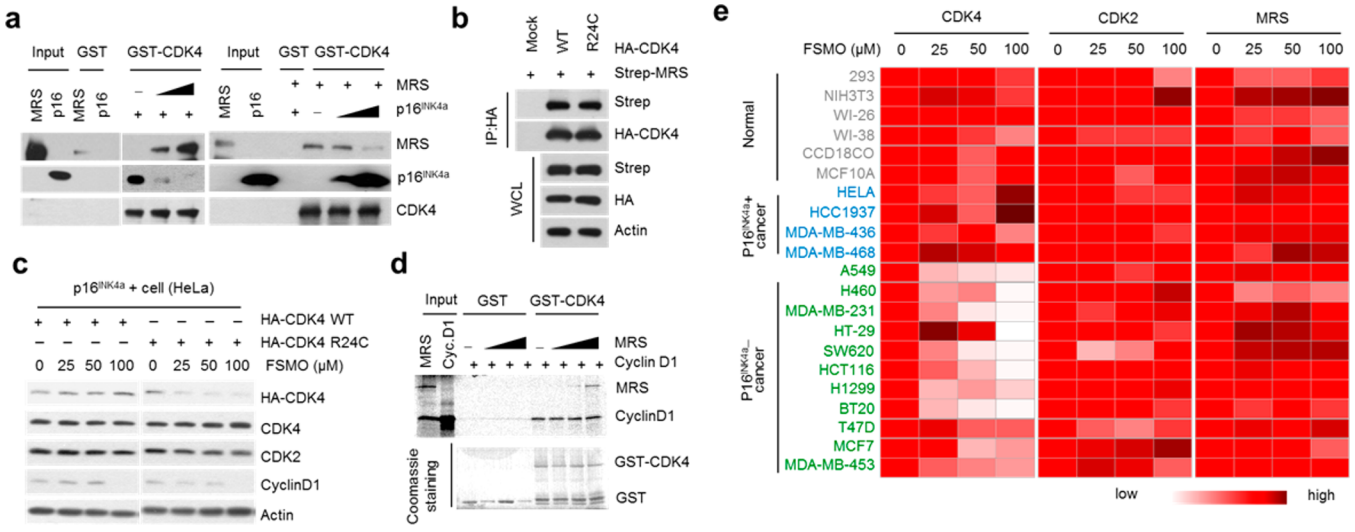

Figure 6. MRS shares an interaction site with p16^{INK4a} for the binding to CDK4 but does not disturb the function of CDK4. (a) Competition between MRS and p16^{INK4a} for the association with CDK4 *in vitro*. (b) Interaction between Strep-MRS and HA-CDK4 R24C mutant. (c) Effect of FSMO on the levels of CDK4 WT and CDK4 R24C mutant. (d) Effect of MRS on the interaction between CDK4 and cyclin D1. (e) Heat map showing the effect of FSMO on CDK4 in normal (gray), p16^{INK4a}-positive cancer (blue), and p16^{INK4a}-negative cancer (green) cell lines. The levels of CDK4, MRS, and CDK2 were investigated via immunoblotting and quantified using ImageJ, and the immunoblotting images are presented in Figure S6c−e.

interaction between the two. The binding motif including D591 and D630 in MRS is in the outer region of the methionyl adenylate binding pocket and linked to the nearby KMSKS loop (Figure 4g,h). As the K596Q mutation abolished the CDK4 interaction, the effect of FSMO on the KMSKS conformation would prevent the CDK4 interaction with MRS.

Effect of MRS on CDK4 Requires HSP90. It is known that the HSP90−CDC37 complex interacts with CDK4 and mediates the proper folding and subsequent release of active CDK4 for the interaction with cyclin D1. Without them, CDK4 falls into degradation pathway.[13,16] To determine whether MRS blocks the proteasome-dependent degradation of CDK4, we investigated the effect of MRS suppression on CDK4 degradation. The reduction of the CDK4 level by MRS knockdown was ablated when the cells were treated with MG132 (Figure 5a), suggesting the involvement of the 26S proteasome in the degradation of CDK4. Both endogenous and exogenous MRS and HSP90 were coimmunoprecipitated with CDK4 (Figure 5b and Figure S5d), suggesting a possible association among MRS, CDK4, and HSP90. A direct interaction of MRS with CDK4 as well as with HSP90, but not with CDC37, was confirmed by GST pull-down assay

DOI: 10.1021/acsptsci.8b00001
ACS Pharmacol. Transl. Sci. 2018, 1, 21−31

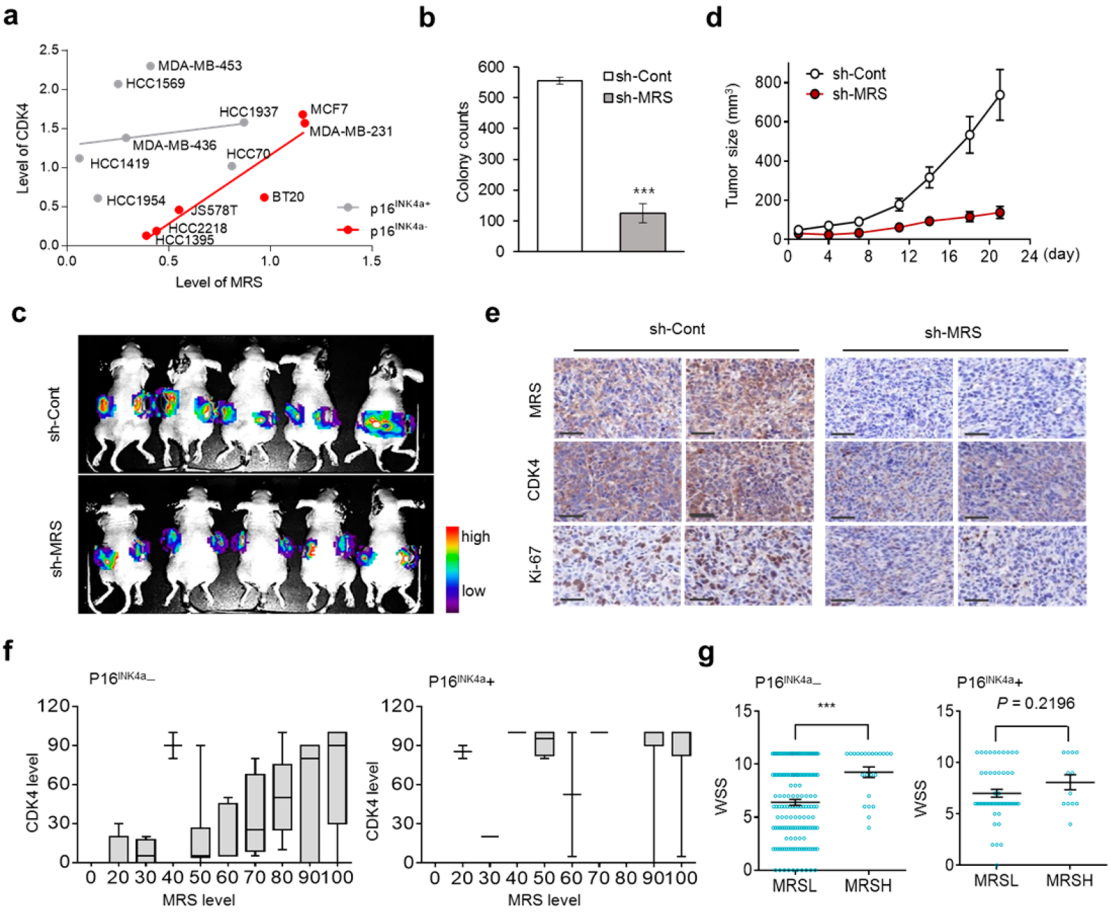

Figure 7. Positive correlation between MRS and CDK4 levels observed in p16^{INK4a}-negative breast cancer. (a) Scatter plot of MRS versus CDK4 protein levels for p16^{INK4a-} (red) and p16^{INK4a+} (gray) breast cancer cell lines. The R^2 values of p16^{INK4a-} and p16^{INK4a+} were 0.8641 and 0.03033, respectively. (b) Anchorage-independent soft agar assay was performed with stable MDA-MB-231 cells with sh-control and sh-MRS (Figure S7a), and the colony numbers are presented (mean ± SEM, n = 3). (***) $P < 0.001$. (c,d) Tumor growth following MRS knockdown in GFP-expressing MDA-MB-231 cells was assayed by fluorescence (c) and tumor size (n = 10) (d). (e) CDK4 and K_i-67 following MRS knockdown in the tumors were assayed by IHC staining. Scale Bar, 50 μm. (f,g) Correlation between MRS and CDK4 (f) and between MRS level and CDK4 signal activation (g) in the absence (n = 171) and presence (n = 75) of p16^{INK4a} in breast cancer (mean ± SEM). (***) $P < 0.001$.

(Figure 5c). To determine whether MRS requires HSP90 for the stabilization of CDK4, we treated cells with the HSP90 inhibitor geldanamycin and compared the CDK4 levels under MRS-overexpressing conditions. Geldanamycin reduced the CDK4 levels even when MRS was overexpressed (Figure 5d), suggesting that HSP90 is required for the MRS-dependent stabilization of CDK4. To investigate the dose-dependent effect of MRS on the intracellular interaction between HSP90 and CDK4, we utilized the nanoBiT (NanoLuc Binary Technology) assay, by which we could quantitate the interaction between HSP90 and CDK4 by measuring reconstituted nanoluciferase luminescence.[30] The luminescence resulting from the association between HSP90 and CDK4 was increased by MRS in a dose-dependent manner, suggesting the positive effect of MRS on the complex formation of CDK4 and HSP90 (Figure 5e). MRS possibly facilitates the interaction of CDK4 with HSP90 by acting as a bridge between the two proteins. MRS suppression and FSMO treatment further disturbed the interaction between CDK4 and HSP90 (Figure 5f), but the levels of other HSP90 clients, CDK7 and p70S6K, were not affected,[14] suggesting that MRS is specific to CDK4.

Dependency of the MRS-CDK4 Interaction on p16^{INK4a}. p16^{INK4a}, an endogenous CDK4 inhibitor, binds to the N-terminus of CDK4, holding CDK4 in an inactive state. p16^{INK4a} competes with HSP90−CDC37 and cyclin D1, although it increases CDK4 stability.[31,32] Since both MRS and p16^{INK4a} can bind to the N-terminal domain of CDK4, they may compete for binding to CDK4. We thus examined this possibility by comparing the CDK4-bound levels of MRS and p16^{INK4a} in the presence of the other. An increase in p16^{INK4a} reduced CDK4 binding to MRS, and the reverse was the same (Figure 6a), indicating that they are in direct competition for the binding to CDK4. Actually, knockdown of p16^{INK4a} increased the intracellular interaction of CDK4 with MRS (Figure S6a), and in the same context, FSMO reduced the CDK4 level only when p16^{INK4a} was reduced by si-RNA in p16^{INK4a}-positive WI-26 cells (Figure S6b). Although MRS and p16^{INK4a} compete with each other to bind CDK4, their binding modes are different because MRS interacted with the CDK4 R24C mutant, which is p16^{INK4a}-binding defective and constitutively active (Figure 6b).[33] In addition, the association between MRS and the CDK4 R24C mutant was hindered by FSMO treatment in p16^{INK4a}-positive cells, unlike that between MRS and CDK4 WT (Figure 6c). These results suggest that the binding site of CDK4 for MRS does not exactly match that of p16^{INK4a}. MRS bound to CDK4 without disturbing the binary interaction between CDK4 and cyclin D1 *in vitro* (Figure 6d), implying that MRS would not affect the

DOI: 10.1021/acsptsci.8b00001
ACS Pharmacol. Transl. Sci. 2018, 1, 21−31

downstream signaling of CDK4, unlike $p16^{INK4a}$. On the basis of these results, the $p16^{INK4a}$-dependent effect of MRS was validated in a broad spectrum of cell lines using FSMO (Figure 6e and Figure S6c−e). FSMO treatment revealed the apparent dose-dependent negative effect on CDK4 levels in $p16^{INK4a}$-negative cancer cells (Figure S6e) compared to that in $p16^{INK4a}$-positive cancer cells (Figure S6d). In addition, $p16^{INK4a}$-negative cancer cells were more sensitive to the antiproliferative effect of FSMO than normal cells or $p16^{INK4a}$-positive cancer cells, indicating a positive correlation with the CDK4 level (Figure S6f). Intriguingly, the FSMO effect was not observed in NIH3T3MEF and MCF10A cells that were $p16^{INK4a}$-negative but not cancerous (Figure S6c),[34,35] implying additional complexity in CDK4 regulation.

Implication of the MRS-CDK4 Relationship in Tumorigenesis. Dysregulation of the cell cycle is one of the most important signatures for tumorigenesis, and the activity of CDK4-cyclin D1 is critical in cancer maintenance as well as in tumor initiation.[7,8] Considering that the CDK4-cyclin D1-pRb axis can depend on MRS, a positive correlation between MRS and CDK4 levels was expected in $p16^{INK4a}$-negative cancer cells. Analysis of the levels of MRS and CDK4 in different breast cancer cell lines revealed that their positive correlation was more apparent in the absence of $p16^{INK4a}$ (Figure 7a). To further investigate the MRS-dependent CDK4 activity in tumorigenesis, we performed anchorage independent soft agar assays using stable MDA-MB-231 cells expressing sh-MRS. MDA-MB-231 cells expressing sh-MRS formed significantly fewer colonies with reduced transformability (Figure 7b and Figure S7a). The sh-MRS-expressing cells showed retarded tumor growth compared to controls in the xenografted mice with no significant reduction in the body weights (Figure 7c,d, and Figure S7b,c). We analyzed the expression of MRS, CDK4, and K_i-67, a proliferation marker, in the xenografts via immunohistochemistry (IHC). The xenografted tumor cells expressing sh-control showed relatively high expression of MRS, CDK4, and K_i-67, but these three factors were reduced in the xenografted tumors of sh-MRS expressing cells (Figure 7e). These results demonstrated that MRS-mediated CDK4 stabilization can modulate cancer cell proliferation. To further validate the relationship between MRS and CDK4 in patient samples, we performed IHC using a tissue microarray containing 246 breast cancer tissues. We analyzed the levels of MRS, CDK4, cyclin D1, pRb (S780), and $p16^{INK4a}$ and classified their levels based on the staining intensity and proportion score (Figure S7d). The percentage of $p16^{INK4a}$-negative cancer was about 69%, and a strong positive correlation between MRS and CDK4 was observed only in these patients (Figure 7f). We further analyzed the relationship of MRS with the downstream factors of CDK4. In this analysis, we gave additional points, commensurate with the sequential activation, to the sum of the CDK4-cyclin D1-pRb scores (Table S2). In this weighted sum of score (WSS), higher values represented the potential signal cascade from MRS to the pRb axis, thus revealing that a high level of MRS was significantly matched with a high WSS only in the $p16^{INK4a}$-negative cases (Figure 7g). These results strongly suggest the significance of the MRS level for the maintenance of CDK4 and its downstream axis in the absence of $p16^{INK4a}$.

In this study, we demonstrated the novel mechanism of MRS, which controls the cell cycle via regulating CDK4 stability. It is worth noting that MRS-mediated CDK4 stabilization was apparent in the absence of $p16^{INK4a}$. Considering that $p16^{INK4a}$ is often altered by deletion, mutation, and epigenetic silencing in various cancers, the MRS dependency of CDK4 could be more significant in cancerous cells.

Amplification of the 12q13−q14 locus harboring the *CDK4* gene occurs in various types of sarcomas, myosarcomas, and osteosarcomas and is significantly associated with poor clinical outcomes compared with amplification of other loci.[36,37] In breast and lung cancers, gene amplification of *CDK4* has been reported to occur at rates of 0.8−15.8% and 1.7−4.3%, respectively.[38−40] Interestingly, CDK4 levels have been observed at much higher frequencies, such as 18.9−70% in breast and 30−50% in lung cancers,[12,39−41] suggesting the existence of an underlying mechanism that can further increase the CDK4 levels after gene expression.

CDC37 and HSP90 form a chaperonic complex for the proper folding of oncogenic kinases, including CDK4, and CDC37 is thought to help the clients for the association with HSP90, albeit its low specificity to each client.[16,42] CDC37 is considered an anticancer target with a potential therapeutic window because of its differential expression between cancer and normal tissues.[13] The high expression of CDC37 has been reported in several cancers, including prostate carcinoma.[13] Whereas prostate cancer is highly associated with the overexpression of CDC37, the correlation between the loss of 16^{INK4a} and a poor prognosis of prostate cancer is controversial,[43−45] suggesting that the activation of the CDK4 pathway is so pervasive in this cancer. Our data show that MRS itself enhances the association between CDK4 and HSP90 in the absence of 16^{INK4a}, implying the CDC37-like role of MRS for the CDK4-HSP90 complex formation (Figure 5e). Unlike CDC37, however, MRS is specific to CDK4 among CDKs and HSP90 clients tested in this study (Figures 1b, 2a, and 5f). It is unclear whether MRS requires the existence of CDC37, and more studies are needed to explain the relationship between MRS and the chaperone complex including CDC37.

Recently, Jia et al. reported that PFKFB3 is important for CDK4 protein turnover by stabilizing the CDK4−HSP90 complex.[46] In this study, the authors analyzed the proteins that coimmunoprecipitated with PFKFB3 via LC−MS/MS and identified CDK4 as well as MRS as the binding partners of PFKFB3. These results agree with those from our study, providing supporting evidence for the MRS and CDK4 interaction, although the authors only focused on the relationship between PFKFB3 and CDK4. Our findings differ from those of Jia et al.[46] in two aspects. First, the MRS and CDK4 interaction mainly occurred in the cytoplasm (Figure 2b and 4d), whereas PFKFB3 and CDK4 interacted within the nucleus. In the cytoplasm, newly synthesized CDK4 requires chaperone proteins to be properly folded and to assemble into productive complexes. Thus, we expect that MRS associates with CDK4 in advance to help complex formation with HSP90 (Figure 5e). Second, MRS-mediated CDK4 regulation is dependent on the presence of $p16^{INK4a}$ unlike PFKFB3. Further work will be needed to explore the differences and relationships between these two mechanisms for CDK4 regulation.

Genetic analysis and mutation studies in yeast revealed that G1 cell cycle arrest was caused by the suppression of translation initiation factors or induction of an MRS loss-of-function mutant.[47,48] These results show that G1 to S transit is more sensitive to translation initiation than other cell cycle phases, giving appropriate prominence for the CDK4 regulation by MRS. However, it was unexpected that the cell cycle is more sensitive to the hypomorphic MRS than protein synthesis. It is

DOI: 10.1021/acsptsci.8b00001
ACS Pharmacol. Transl. Sci. 2018, 1, 21−31

worth noting that MRS links translational inhibition to DNA repair under UV stress, which is one of the checkpoints of the cell cycle.[20] Following UV stress, MRS releases its binding partner, AIMP3, so that AIMP3 can execute DNA repair in the nucleus. These data imply the close connection of translation with cell cycle control and that MRS is one of the molecules that send cues to cell cycle-regulating factors in response to stimuli.

FSMO inhibits the MRS−CDK4 interaction at relatively low concentrations, and in addition, FSMO suppresses MRS activity at high concentrations, implying that FSMO cannot perfectly substitute for Met. Considering that the Km value of Met to MRS was about 100 μM,[49] the requirement for a high concentration of FSMO to inhibit the MRS catalytic activity can be reasonably accepted. On the basis of the docking model, the MRS−CDK4 interacting surface is not the direct catalytic site but links close to the KMSKS motif (Figure 4g,h), and the conformational change induced by MRS modulators seems to be important for disturbing the interaction. This structural information may help to design MRS-targeting compounds. In this study, we showed that the cell cycle can be specifically regulated via MRS without affecting its catalytic activity, while catalytic inhibitors of MRS can also induce cell death.[50] Thus, MRS can provide dual target points, one through its catalytic activity and the other through its role in CDK4 regulation. Depending on genetic and environmental characteristics, either or both of these two routes can be explored to control cancer.

METHODS

Cell Lines, Plasmids, and si-RNA. MDA-MD-231, 293, 293T, NIH3T3, WI-26, WI-38, CCD18C0, and HeLa cells were purchased from the American Type Culture Collection (ATCC), and BT20, MCF7, HT29, and T47D cells were obtained from the Korean Cell Line Bank (KCLB). GFP-expressing MDA-MB-231 cells were purchased from Cell Biolabs. These cells were maintained using DMEM (Hyclone) supplemented with heat-inactivated 10% dFBS (defined fetal bovine serum) and 50 μg/mL penicillin/streptomycin in 5% CO_2 at 37 °C. CHO-K1 cells were purchased from the ATCC, and HCC1937, MDA-MB-453, MDA-MB-436, MDA-MB-468, A549, H460, HCT116, H1299, and SW620 cells were purchased from the KCLB and cultured using RPMI supplemented with 10% FBS and 50 μg/mL penicillin/streptomycin. MCF10A cells were maintained using DMEM/F12 media with 10 μg/mL insulin, 100 ng/mL cholera toxin, 25 ng/mL epidermal growth factor, 500 ng/mL hydrocortisone, 0.2% (v/v) amphotericin B, 5% horse serum, and 50 μg/mL penicillin/streptomycin.

MRS, CDK4, HSP90, CDC37, and LRS were cloned into pcDNA3 (Invitrogen). A Myc or Flag tag was fused to the N-terminus region of each insert, and an HA tag was fused in the C-terminus region of each insert. The pEXPR IBA105 plasmid (IBA) was used for the cloning with the strep tag. Plasmids and siRNAs were transfected using FuGENE HD (Roche) and Lipofectamine 2000 (Invitrogen), respectively, according to the manufacturer's instructions. The sequences for si-MRS and si-$p16^{INK4a}$ are 5′-CUACCGCUGGUUUAACAUUUCGUUU-3′ and 5′-CGCACCGAATAGTTACGGT-3′, respectively.

Proteins, Antibodies, and Met Analogues. Purified human $p16^{INK4a}$ protein was purchased from Sigma (SRP3134). Primary antibodies for HA (mouse, sc-7392; Santa Cruz and rabbit, H6908; Sigma), Myc (mouse, sc-40; Santa Cruz), Flag (mouse, F3165; Sigma), Strep-HRP (2-1509-001; IBA), tubulin (mouse, T6074; Sigma), β-actin (mouse, A1978; Sigma), CDK4 (mouse, sc-23896 and rabbit, sc-260; Santa Cruz), cyclin D1 (rabbit, 04-221; Merckmillipore), p-Rb (rabbit, #3590; Cell Signaling), HSP90α/β (rabbit, sc-7947; Santa Cruz), CDC37 (rabbit, sc-5617; Santa Cruz), p16 (rabbit, sc-468; Santa Cruz), CDK3 (rabbit, sc-28256; Santa Cruz), CDK6 (mouse, sc-7961; Santa Cruz), and MRS (mouse, ab50793; Abcam) and a CDK antibody sampler kit (#9868; Cell Signaling) and a Cyclin antibody sampler kit (#9869; Cell Signaling) were used to perform immunoblotting, immunoprecipitation, and immunofluorescence staining. Met analogues including FSMO were purchased from AnaSpec.

Stable Cell Line Preparation. MDA-MB-231 or GFP-expressing MDA-MB-231 cells were transfected with Smart choice inducible lentivirus (GE Healthcare), which encodes the sh-MRS RNA (5′-TAGATCCAAGAGTTTCGCC-3′). After lentivirus transduction, stable cells were selected under puromycin pressure (1 μg/mL), and colonies were picked for further analysis. Sh-MRS and sh-control expression was induced by doxycycline treatment (1 μg/mL) at least for 3 d before the experiment.

Cell Cycle Analysis with FACS. Cells were harvested by trypsinization, washed twice with cold PBS, and fixed in 70% ethanol for 2 h at 4 °C. After fixation, the cells were washed twice with cold PBS and incubated in 500 μL PI (propidium iodide) staining solution [1 × PBS, 100 μg/mL RNase A, and 50 μg/mL PI (Sigma-Aldrich)] for 30 min at 37 °C in the dark. The samples were analyzed by flow cytometry (BD Biosciences). The percentages of cells in the G0/G1, S, and G2/M phases were analyzed using Cell Quest acquisition software (BD Biosciences).

BrdU Incorporation Assay. MDA-MB-231 and H460 cells were seeded in 96-well plates at a density of 4000 cells per well. After adhesion, cells were treated with 50 μM FSMO for 8 h in 2% serum media. For MRS knockdown, sh-MRS in the MDA-MB-231 cells were induced with doxycycline (1 μg/mL) for 72 h, and H460 cells were transfected with si-MRS for 72 h. BrdU solution (100 μL) in 2% serum medium was added to each well for a 2 h incubation. Cells were fixed and treated with antibodies according to the guidelines in the cell proliferation assay kit (Cell Signaling). Finally, the plates were washed three times with wash buffer, and 100 μL of tetramethylbenzidine (TMB) substrate was added followed by incubation for 30 s at room temperature (RT). The amount of BrdU incorporated into the cells was determined at 450 nm by an ELISA reader (Tecan).

Cell Viability Analysis with IncuCyte. Cells were seeded at 2000 cells/well in 96 well plate and incubated. The next day, media were replaced with corresponding media containing 5% dFBS and different concentrations of FSMO, and then, growth was monitored using the IncuCyte Kinetic Live Cell Imaging System (Essen BioScience). To calculate the GI_{50} value (the concentration for 50% of maximal inhibition of cell proliferation), cells were treated with FSMO at different concentrations and incubated for 3 d. The GI_{50} value was calculated using Prism 5 software (GraphPad).

Stable MDA-MB-231 or H460 cells were transfected with pcDNA3-empty vector, pcDNA3-CDK4, pEXPR-IBA105-MRS, pEXPR-IBA105-CDK4, or pcDNA3-LRS, and the cell growth rate was monitored.

Firefly Luciferase *in Vitro* Translation Assay. *In vitro* translation assay was performed using rabbit reticulocyte lysate (Promega). The reaction mixture [1 μL of template (0.5 mg/

DOI: 10.1021/acsptsci.8b00001
ACS Pharmacol. Transl. Sci. 2018, 1, 21−31

mL firefly luciferase DNA), 1 μL of FSMO compound (AnaSpec) with different stock concentrations, 6 μL of rabbit reticulocyte lysate, and DW up to 10 μL] was prepared and incubated at 30 °C for 1.5 h. To monitor the translation recovery in the presence of excess amino acids, 1 μL of each amino acid (Met, Ser, Cys, and Leu, 100 mM stock) was added to the reaction sample. After incubation, 10 μL of 2× luciferase substrate was added to the mixture. The luciferase signal was measured by the GloMax Discover System (Promega).

Statistical Analysis. All statistical analyses and generation of graphs were performed using Prism 5 software (GraphPad), including Student's *t* tests.

■ ASSOCIATED CONTENT

Supporting Information

The Supporting Information is available free of charge on the ACS Publications website at DOI: 10.1021/acsptsci.8b00001.

Additional materials and methods; figures; tables; raw data for immunoblotting (PDF)

■ AUTHOR INFORMATION

Corresponding Author

*E-mail: sungkim@snu.ac.kr.

ORCID

Basappa: 0000-0002-6810-9219

Sunghoon Kim: 0000-0002-1570-3230

Author Contributions

○N.H.K. and J.Y.L. contributed equally to this work. N.H.K. and S.K designed the study. N.H.K., J.Y.L., Y.L.Y, C.K., J.K., S.O., H.W.A., S.G.A., H.K.K., J.H.K., D.Y.H., M.C.P., D.K., R.T., I.M., and Y.K. performed the experiments. B.S.K., J.J., Y.M.H., S.I.J., Y.S.C., D.K.L., Y.K., M.W.W., B., and S.K. analyzed and interpreted the data. N.H.K., J.Y.L., B.S.K., Y.K., and S.K. wrote the paper. All authors reviewed and commented on the manuscript.

Notes

The authors declare no competing financial interest.

■ ACKNOWLEDGMENTS

This work is supported by the Ministry of Health & Welfare (HI13C21480301), the Korea Health Technology R&D Project. It was also funded and by NRF-M3A6A4-2010-0029785, NRF-2015M3A6A4065724, and NRF-2017M3A9F7079378, National Research Foundation funded by the Ministry of Science and ICT of Korea. This study was also supported by Gyeonggi Research Development Program.

■ REFERENCES

(1) Musgrove, E. A., Caldon, C. E., Barraclough, J., Stone, A., and Sutherland, R. L. (2011) Cyclin D as a therapeutic target in cancer. *Nat. Rev. Cancer 11*, 558−572.

(2) Kitagawa, M., Higashi, H., Jung, H. K., Suzuki-Takahashi, I., Ikeda, M., Tamai, K., Kato, J., Segawa, K., Yoshida, E., Nishimura, S., and Taya, Y. (1996) The consensus motif for phosphorylation by cyclin D1-Cdk4 is different from that for phosphorylation by cyclin A/E-Cdk2. *EMBO J. 15*, 7060−7069.

(3) Rane, S. G., Dubus, P., Mettus, R. V., Galbreath, E. J., Boden, G., Reddy, E. P., and Barbacid, M. (1999) Loss of Cdk4 expression causes insulin-deficient diabetes and Cdk4 activation results in beta-islet cell hyperplasia. *Nat. Genet. 22*, 44−52.

(4) Berthet, C., Klarmann, K. D., Hilton, M. B., Suh, H. C., Keller, J. R., Kiyokawa, H., and Kaldis, P. (2006) Combined loss of Cdk2 and Cdk4 results in embryonic lethality and Rb hypophosphorylation. *Dev. Cell 10*, 563−573.

(5) Yu, Q., Sicinska, E., Geng, Y., Ahnstrom, M., Zagozdzon, A., Kong, Y., Gardner, H., Kiyokawa, H., Harris, L. N., Stal, O., and Sicinski, P. (2006) Requirement for CDK4 kinase function in breast cancer. *Cancer Cell 9*, 23−32.

(6) Zou, X., Ray, D., Aziyu, A., Christov, K., Boiko, A. D., Gudkov, A. V., and Kiyokawa, H. (2002) Cdk4 disruption renders primary mouse cells resistant to oncogenic transformation, leading to Arf/p53-independent senescence. *Genes Dev. 16*, 2923−2934.

(7) Reddy, H. K., Mettus, R. V., Rane, S. G., Grana, X., Litvin, J., and Reddy, E. P. (2005) Cyclin-dependent kinase 4 expression is essential for neu-induced breast tumorigenesis. *Cancer Res. 65*, 10174−10178.

(8) Malumbres, M., and Barbacid, M. (2009) Cell cycle, CDKs and cancer: a changing paradigm. *Nat. Rev. Cancer 9*, 153−166.

(9) Turner, N. C., Ro, J., Andre, F., Loi, S., Verma, S., Iwata, H., Harbeck, N., Loibl, S., Huang Bartlett, C., Zhang, K., Giorgetti, C., Randolph, S., Koehler, M., and Cristofanilli, M. (2015) Palbociclib in Hormone-Receptor-Positive Advanced Breast Cancer. *N. Engl. J. Med. 373*, 209−219.

(10) Witkiewicz, A. K., Knudsen, K. E., Dicker, A. P., and Knudsen, E. S. (2011) The meaning of p16(ink4a) expression in tumors: functional significance, clinical associations and future developments. *Cell Cycle 10*, 2497−2503.

(11) Casimiro, M. C., Velasco-Velazquez, M., Aguirre-Alvarado, C., and Pestell, R. G. (2014) Overview of cyclins D1 function in cancer and the CDK inhibitor landscape: past and present. *Expert Opin. Invest. Drugs 23*, 295−304.

(12) Wu, A., Wu, B., Guo, J., Luo, W., Wu, D., Yang, H., Zhen, Y., Yu, X., Wang, H., Zhou, Y., Liu, Z., Fang, W., and Yang, Z. (2011) Elevated expression of CDK4 in lung cancer. *J. Transl. Med. 9*, 38.

(13) Gray, P. J., Jr., Prince, T., Cheng, J., Stevenson, M. A., and Calderwood, S. K. (2008) Targeting the oncogene and kinome chaperone CDC37. *Nat. Rev. Cancer 8*, 491−495.

(14) Taipale, M., Krykbaeva, I., Koeva, M., Kayatekin, C., Westover, K. D., Karras, G. I., and Lindquist, S. (2012) Quantitative analysis of HSP90-client interactions reveals principles of substrate recognition. *Cell 150*, 987−1001.

(15) Smith, J. R., de Billy, E., Hobbs, S., Powers, M., Prodromou, C., Pearl, L., Clarke, P. A., and Workman, P. (2015) Restricting direct interaction of CDC37 with HSP90 does not compromise chaperoning of client proteins. *Oncogene 34*, 15−26.

(16) Trepel, J., Mollapour, M., Giaccone, G., and Neckers, L. (2010) Targeting the dynamic HSP90 complex in cancer. *Nat. Rev. Cancer 10*, 537−549.

(17) Kim, S., You, S., and Hwang, D. (2011) Aminoacyl-tRNA synthetases and tumorigenesis: more than housekeeping. *Nat. Rev. Cancer 11*, 708−718.

(18) Lee, J. Y., Kim, D. G., Kim, B. G., Yang, W. S., Hong, J., Kang, T., Oh, Y. S., Kim, K. R., Han, B. W., Hwang, B. J., Kang, B. S., Kang, M. S., Kim, M. H., Kwon, N. H., and Kim, S. (2014) Promiscuous methionyl-tRNA synthetase mediates adaptive mistranslation to protect cells against oxidative stress. *J. Cell Sci. 127*, 4234−4245.

(19) Wiltrout, E., Goodenbour, J. M., Frechin, M., and Pan, T. (2012) Misacylation of tRNA with methionine in Saccharomyces cerevisiae. *Nucleic Acids Res. 40*, 10494−10506.

(20) Kwon, N. H., Kang, T., Lee, J. Y., Kim, H. H., Kim, H. R., Hong, J., Oh, Y. S., Han, J. M., Ku, M. J., Lee, S. Y., and Kim, S. (2011) Dual role of methionyl-tRNA synthetase in the regulation of translation and tumor suppressor activity of aminoacyl-tRNA synthetase-interacting multifunctional protein-3. *Proc. Natl. Acad. Sci. U. S. A. 108*, 19635−19640.

(21) Ko, Y. G., Kang, Y. S., Kim, E. K., Park, S. G., and Kim, S. (2000) Nucleolar localization of human methionyl-tRNA synthetase and its role in ribosomal RNA synthesis. *J. Cell Biol. 149*, 567−574.

(22) Frechin, M., Enkler, L., Tetaud, E., Laporte, D., Senger, B., Blancard, C., Hammann, P., Bader, G., Clauder-Munster, S., Steinmetz, L. M., Martin, R. P., di Rago, J. P., and Becker, H. D. (2014) Expression of nuclear and mitochondrial genes encoding ATP

synthase is synchronized by disassembly of a multisynthetase complex. *Mol. Cell 56*, 763−776.
(23) Hadchouel, A., Wieland, T., Griese, M., Baruffini, E., Lorenz-Depiereux, B., Enaud, L., Graf, E., Dubus, J. C., Halioui-Louhaichi, S., Coulomb, A., Delacourt, C., Eckstein, G., Zarbock, R., Schwarzmayr, T., Cartault, F., Meitinger, T., Lodi, T., de Blic, J., and Strom, T. M. (2015) Biallelic Mutations of Methionyl-tRNA Synthetase Cause a Specific Type of Pulmonary Alveolar Proteinosis Prevalent on Reunion Island. *Am. J. Hum. Genet. 96*, 826−831.
(24) Gonzalez, M., McLaughlin, H., Houlden, H., Guo, M., Yo-Tsen, L., Hadjivassilious, M., Speziani, F., Yang, X. L., Antonellis, A., Reilly, M. M., and Zuchner, S. (2013) Exome sequencing identifies a significant variant in methionyl-tRNA synthetase (MARS) in a family with late-onset CMT2. *J. Neurol., Neurosurg. Psychiatry 84*, 1247−1249.
(25) van Meel, E., Wegner, D. J., Cliften, P., Willing, M. C., White, F. V., Kornfeld, S., and Cole, F. S. (2013) Rare recessive loss-of-function methionyl-tRNA synthetase mutations presenting as a multi-organ phenotype. *BMC Med. Genet. 14*, 106.
(26) Friedel, R. H., and Soriano, P. (2010) Gene trap mutagenesis in the mouse. *Methods Enzymol. 477*, 243−269.
(27) Alao, J. P. (2007) The regulation of cyclin D1 degradation: roles in cancer development and the potential for therapeutic invention. *Mol. Cancer 6*, 24.
(28) Fourmy, D., Mechulam, Y., Brunie, S., Blanquet, S., and Fayat, G. (1991) Identification of residues involved in the binding of methionine by Escherichia coli methionyl-tRNA synthetase. *FEBS Lett. 292*, 259−263.
(29) Mechulam, Y., Dardel, F., Le Corre, D., Blanquet, S., and Fayat, G. (1991) Lysine 335, part of the KMSKS signature sequence, plays a crucial role in the amino acid activation catalysed by the methionyl-tRNA synthetase from Escherichia coli. *J. Mol. Biol. 217*, 465−475.
(30) Dixon, A. S., Schwinn, M. K., Hall, M. P., Zimmerman, K., Otto, P., Lubben, T. H., Butler, B. L., Binkowski, B. F., Machleidt, T., Kirkland, T. A., Wood, M. G., Eggers, C. T., Encell, L. P., and Wood, K. V. (2016) NanoLuc Complementation Reporter Optimized for Accurate Measurement of Protein Interactions in Cells. *ACS Chem. Biol. 11*, 400−408.
(31) Bockstaele, L., Coulonval, K., Kooken, H., Paternot, S., and Roger, P. P. (2006) Regulation of CDK4. *Cell Div. 1*, 25.
(32) Stepanova, L., Finegold, M., DeMayo, F., Schmidt, E. V., and Harper, J. W. (2000) The oncoprotein kinase chaperone CDC37 functions as an oncogene in mice and collaborates with both c-myc and cyclin D1 in transformation of multiple tissues. *Mol. Cell. Biol. 20*, 4462−4473.
(33) Sotillo, R., Dubus, P., Martin, J., de la Cueva, E., Ortega, S., Malumbres, M., and Barbacid, M. (2001) Wide spectrum of tumors in knock-in mice carrying a Cdk4 protein insensitive to INK4 inhibitors. *EMBO J. 20*, 6637−6647.
(34) Debnath, J., Muthuswamy, S. K., and Brugge, J. S. (2003) Morphogenesis and oncogenesis of MCF-10A mammary epithelial acini grown in three-dimensional basement membrane cultures. *Methods 30*, 256−268.
(35) Ikeda, H., Yoshida, J., Yamada, H., Yoshimatsu, T., and Ikenaka, K. (1997) Retroviral introduction of the p16 gene into murine cell lines to elicit marked antiproliferative effects. *Jpn. J. Cancer Res. 88*, 712−717.
(36) Barr, F. G., Duan, F., Smith, L. M., Gustafson, D., Pitts, M., Hammond, S., and Gastier-Foster, J. M. (2009) Genomic and clinical analyses of 2p24 and 12q13-q14 amplification in alveolar rhabdomyosarcoma: a report from the Children's Oncology Group. *Genes, Chromosomes Cancer 48*, 661−672.
(37) Mejia-Guerrero, S., Quejada, M., Gokgoz, N., Gill, M., Parkes, R. K., Wunder, J. S., and Andrulis, I. L. (2010) Characterization of the 12q15 MDM2 and 12q13−14 CDK4 amplicons and clinical correlations in osteosarcoma. *Genes, Chromosomes Cancer 49*, 518−525.
(38) Forbes, S. A., Beare, D., Gunasekaran, P., Leung, K., Bindal, N., Boutselakis, H., Ding, M., Bamford, S., Cole, C., Ward, S., Kok, C. Y., Jia, M., De, T., Teague, J. W., Stratton, M. R., McDermott, U., and Campbell, P. J. (2015) COSMIC: exploring the world's knowledge of somatic mutations in human cancer. *Nucleic Acids Res. 43*, D805−811.
(39) Peurala, E., Koivunen, P., Haapasaari, K. M., Bloigu, R., and Jukkola-Vuorinen, A. (2013) The prognostic significance and value of cyclin D1, CDK4 and p16 in human breast cancer. *Breast Cancer Res. 15*, R5.
(40) An, H. X., Beckmann, M. W., Reifenberger, G., Bender, H. G., and Niederacher, D. (1999) Gene amplification and overexpression of CDK4 in sporadic breast carcinomas is associated with high tumor cell proliferation. *Am. J. Pathol. 154*, 113−118.
(41) Wikman, H., Nymark, P., Vayrynen, A., Jarmalaite, S., Kallioniemi, A., Salmenkivi, K., Vainio-Siukola, K., Husgafvel-Pursiainen, K., Knuutila, S., Wolf, M., and Anttila, S. (2005) CDK4 is a probable target gene in a novel amplicon at 12q13.3-q14.1 in lung cancer. *Genes, Chromosomes Cancer 42*, 193−199.
(42) Roe, S. M., Ali, M. M., Meyer, P., Vaughan, C. K., Panaretou, B., Piper, P. W., Prodromou, C., and Pearl, L. H. (2004) The Mechanism of Hsp90 regulation by the protein kinase-specific cochaperone p50(cdc37). *Cell 116*, 87−98.
(43) Remo, A., Pancione, M., Zanella, C., and Manfrin, E. (2016) p16 Expression in Prostate Cancer and Nonmalignant Lesions: Novel Findings and Review of the Literature. *Appl. Immunohistochem. Mol. Morphol. 24*, 201−206.
(44) Burdelski, C., Dieckmann, T., Heumann, A., Hube-Magg, C., Kluth, M., Beyer, B., Steuber, T., Pompe, R., Graefen, M., Simon, R., Minner, S., Tsourlakis, M. C., Koop, C., Izbicki, J., Sauter, G., Krech, T., Schlomm, T., Wilczak, W., and Lebok, P. (2016) p16 upregulation is linked to poor prognosis in ERG negative prostate cancer. *Tumor Biol. 37*, 12655−12663.
(45) Chakravarti, A., DeSilvio, M., Zhang, M., Grignon, D., Rosenthal, S., Asbell, S. O., Hanks, G., Sandler, H. M., Khor, L. Y., Pollack, A., and Shipley, W. (2007) Prognostic value of p16 in locally advanced prostate cancer: a study based on Radiation Therapy Oncology Group Protocol 9202. *J. Clin. Oncol. 25*, 3082−3089.
(46) Jia, W., Zhao, X., Zhao, L., Yan, H., Li, J., Yang, H., Huang, G., and Liu, J. (2018) Non-canonical roles of PFKFB3 in regulation of cell cycle through binding to CDK4. *Oncogene 37*, 1685−1698.
(47) Unger, M. W., and Hartwell, L. H. (1976) Control of cell division in Saccharomyces cerevisiae by methionyl-tRNA. *Proc. Natl. Acad. Sci. U. S. A. 73*, 1664−1668.
(48) Polymenis, M., and Aramayo, R. (2015) Translate to divide: control of the cell cycle by protein synthesis. *Microbial Cell 2*, 94−104.
(49) Green, L. S., Bullard, J. M., Ribble, W., Dean, F., Ayers, D. F., Ochsner, U. A., Janjic, N., and Jarvis, T. C. (2009) Inhibition of methionyl-tRNA synthetase by REP8839 and effects of resistance mutations on enzyme activity. *Antimicrob. Agents Chemother. 53*, 86−94.
(50) Bharathkumar, H., Mohan, C. D., Rangappa, S., Kang, T., Keerthy, H. K., Fuchs, J. E., Kwon, N. H., Bender, A., Kim, S., Basappa, and Rangappa, K. S. (2015) Screening of quinoline, 1,3-benzoxazine, and 1,3-oxazine-based small molecules against isolated methionyl-tRNA synthetase and A549 and HCT116 cancer cells including an in silico binding mode analysis. *Org. Biomol. Chem. 13*, 9381−9387.

DOI: 10.1021/acsptsci.8b00001
ACS Pharmacol. Transl. Sci. 2018, 1, 21−31